Received: 30 March 2021 | Accepted: 31 March 2021

DOI: 10.1111/gtc.12847

ORIGINAL ARTICLE

Genes to Cells WILEY

Sonic hedgehog expands neural stem cells in the neocortical region leading to an expanded and wrinkled neocortical surface

Mohammed Shqirat[1,2] | **Akira Kinoshita**[1,3] | **Ryoichiro Kageyama**[1,2,3,4,5] | **Toshiyuki Ohtsuka**[1,2,3]

[1]Institute for Frontier Life and Medical Sciences, Kyoto University, Kyoto, Japan

[2]Graduate School of Medicine, Kyoto University, Kyoto, Japan

[3]Graduate School of Biostudies, Kyoto University, Kyoto, Japan

[4]Institute for Integrated Cell-Material Sciences (iCeMS), Kyoto University, Kyoto, Japan

[5]RIKEN Center for Brain Science, Wako, Japan

Correspondence
Toshiyuki Ohtsuka, Institute for Frontier Life and Medical Sciences, Kyoto University, 53 Kawahara-cho, Shogoin, Sakyo-ku, Kyoto 606-8507, Japan.
Email: tohtsuka@infront.kyoto-u.ac.jp

Funding information
Core Research for Evolutional Science and Technology, Grant/Award Number: JPMJCR12W2; Ministry of Education, Culture, Sports, Science and Technology (MEXT), Grant/Award Number: 16H06480; Japan Society for the Promotion of Science, Grant/Award Number: 15K06773 and 18K06253

Communicated by: Tadashi Uemura

Abstract

An expanded and folded neocortex is characteristic of higher mammals, including humans and other primates. The neocortical surface area was dramatically enlarged during the course of mammalian brain evolution from lissencephalic to gyrencephalic mammals, and this bestowed higher cognitive functions especially to primates, including humans. In this study, we generated transgenic (Tg) mice in which the expression of Sonic hedgehog (Shh) could be controlled in neural stem cells (NSCs) and neural progenitors by using the Tet-on system. Shh overexpression during embryogenesis promoted the symmetric proliferative division of NSCs in the neocortical region, leading to the expansion of lateral ventricles and tangential extension of the ventricular zone. Moreover, Shh-overexpressing Tg mice showed dramatic expansion of the neocortical surface area and exhibited a wrinkled brain when overexpression was commenced at early stages of neural development. These results indicate that Shh is able to increase the neocortical NSCs and contribute to expansion of the neocortex.

KEYWORDS

brain morphogenesis, mouse, neocortical development, neural stem cell, neurogenesis, Sonic hedgehog

1 | INTRODUCTION

During mammalian brain evolution, the neocortex was dramatically enlarged and adopted a wrinkled shape to accommodate the expanded neocortical surface inside the skull in gyrencephalic mammals (Sun & Hevner, 2014). Sonic hedgehog (Shh) signaling governs various aspects of the development of the central nervous system (CNS), including dorso-ventral (D-V) patterning of the neural tube (Echelard et al., 1993; Fuccillo et al., 2006; Patten & Placzek, 2000) and the proliferation of neural progenitors in the cerebellum (Wallace, 1999). In the telencephalon, *Shh* is highly expressed in the floor plate, and the secreted Shh proteins form a ventral-high-dorsal-low gradient and play a key role in establishing ventral identity (Chiang et al., 1996; Dale et al., 1997; Ericson et al., 1995). Shh proteins can be delivered dorsally through

the cerebrospinal fluid (CSF) in the brain vesicles (ventricles). In addition, it is known that Shh is produced in the dorsal telencephalon and influences the neocortical development (Dave et al., 2011; Komada et al., 2008, 2013; Yabut & Pleasure, 2018). It has also been reported that Shh signaling regulates the proliferation of neural stem cells (NSCs) and controls their number during neocortical development (Palma & Ruiz i Altaba, 2004).

Here, we generated transgenic (Tg) mice in which Shh expression can be controlled in NSCs and neural progenitors throughout the CNS using the Tet-on system and revealed that its overexpression enhances the maintenance and proliferation of NSCs in the developing neocortical region. Shh-overexpressing Tg mice exhibited a dramatic enlargement of the neocortical surface area and a wrinkled neocortex when Shh expression was induced from the early stages of neural development.

2 | RESULTS AND DISCUSSION

2.1 | Overexpression of Shh increased NSCs and expanded the ventricular zone in the neocortical region

To investigate the impact of Shh on neocortical development, we performed in utero electroporation to overexpress Shh in NSCs in the ventricular zone (VZ). *pCAG-Shh* combined with *pCAG-EGFP* or *pCAG-EGFP* alone (as a control) was transfected into the VZ cells at embryonic day 13.5 (E13.5), and brains were fixed and analyzed at E16.5. Immunohistochemical staining was performed using antibodies against EGFP, Pax6, a marker for NSCs, Tbr2, a marker for intermediate progenitor cells (IPCs), and Tuj1, a marker for neurons. As shown in the top panels of Figure 1a, expression vectors were introduced in the VZ of the dorsolateral telencephalon (neocortical region) of the unilateral hemisphere on the anode side and the VZ of the medial regions of the contralateral hemisphere on the cathode side. It was observed that $Pax6^+$ NSCs and $Tbr2^+$ IPCs were increased in number and the VZ/subventricular zone (SVZ) was expanded in the neocortical region transfected with Shh expression vectors, compared to the corresponding region transfected with control vectors (Figure 1a,b,d).

We next estimated the cell proliferation rate by 5-bromo-2′-deoxyuridine (BrdU) incorporation experiments. BrdU was intraperitoneally injected into pregnant mice 30 min before sacrifice at E16.5 to mark cells that incorporated BrdU in the S phase. The numbers of $BrdU^+$ cells and cells positive for Ki67, a marker for proliferating cells, were remarkably increased in the VZ/SVZ around the electroporated regions (Figure 1c,d). The proportions of $Pax6^+$, $Tbr2^+$, $BrdU^+$ and $Ki67^+$ cells among GFP^+ cells were also increased, except for the fact that the increase in the proportion of $Tbr2^+$ cells was not significant, indicating that transient overexpression of Shh promoted the maintenance and proliferation of NSCs through a cell autonomous and/or paracrine effect (Figure 1d). We then analyzed the division mode of transfected cells by referring to previous reports (Wang et al., 2016; Watanabe et al., 2015). EdU was injected intraperitoneally into pregnant mice and the proportions of $Pax6^+$; EdU^+/EdU^+ cells and $Tbr2^+$; EdU^+/EdU^+ cells were evaluated 18 hr later during the period between cell division and reentry into the S phase, based on the estimated cell cycle length. We observed that NSCs transfected with Shh expression vectors continued the expansion of $Pax6^+$ cells via symmetric proliferative divisions, whereas significantly more NSCs transfected with control vectors produced $Tbr2^+$ IPCs through asymmetric neurogenic divisions at E14.5 (Figure 1e).

2.2 | Shh-overexpressing mice exhibited expanded ventricles and a wrinkled neocortex

Based on the results of in utero electroporation, we aimed to generate Tg mice in which mouse Shh (mShh) expression in NSCs and neural progenitors could be controlled using the Tet-on system. We generated *TRE-mShh/d2EGFP* Tg mice (Figure 2a) and crossed them with *pNes-rtTA* Tg mice (Bansod et al., 2017). In these double Tg mice, Shh and d2E-GFP were expressed throughout the CNS, including the brain

FIGURE 1 Increase in NSCs and expansion of the VZ by transient overexpression of Shh. (a and b) Immunohistochemical analysis to estimate the effects of Shh overexpression on $Pax6^+$ NSCs (a) and $Tbr2^+$ IPCs (b). *pCAG-Shh* together with *pCAG-EGFP* or *pCAG-EGFP* alone [as a control (CTRL)] was introduced into the VZ cells of mouse embryos via in utero electroporation at E13.5, and mice were sacrificed and analyzed at E16.5. Immunostaining was performed with anti-GFP (green), anti-Pax6 (in a) or anti-Tbr2 (in b) (red) and anti-Tuj1 (green) antibodies on coronal sections of the telencephalon. (a) The boxed areas in upper panels are magnified in lower panels. Transfected cells (GFP^+) were observed in unilateral neocortical region on the anode (+) side (white arrows) and medial region of the contralateral hemisphere on the cathode (−) side. (c) Coronal sections of the neocortical region were immunostained using anti-GFP (green) and anti-BrdU or anti-Ki67 (red) antibodies. BrdU was injected intraperitoneally into the pregnant mice 30 min before sacrifice. (d) The numbers of $Pax6^+$, $Tbr2^+$, $BrdU^+$ and $Ki67^+$ cells within a radial column of 200 μm width in electroporated regions (left) and the proportions of $Pax6^+$, $Tbr2^+$, $BrdU^+$ and $Ki67^+$ cells among GFP^+ cells (right). (e) Analysis of the division mode of transfected cells. In utero electroporation was performed at E13.5, and EdU was injected intraperitoneally into pregnant mice 12 hr after in utero electroporation. Proportions of $Pax6^+$; EdU^+/EdU^+ cells and $Tbr2^+$; EdU^+/EdU^+ cells were estimated 18 hr after EdU injection at E14.5. Data are mean ± *SEM* ($n = 4$); $^*p < .05$, $^{**}p < .01$, $^{***}p < .001$ (Student's *t* test). Scale bars: 1 mm in a (upper panels); 200 μm in a (lower panels), b, c

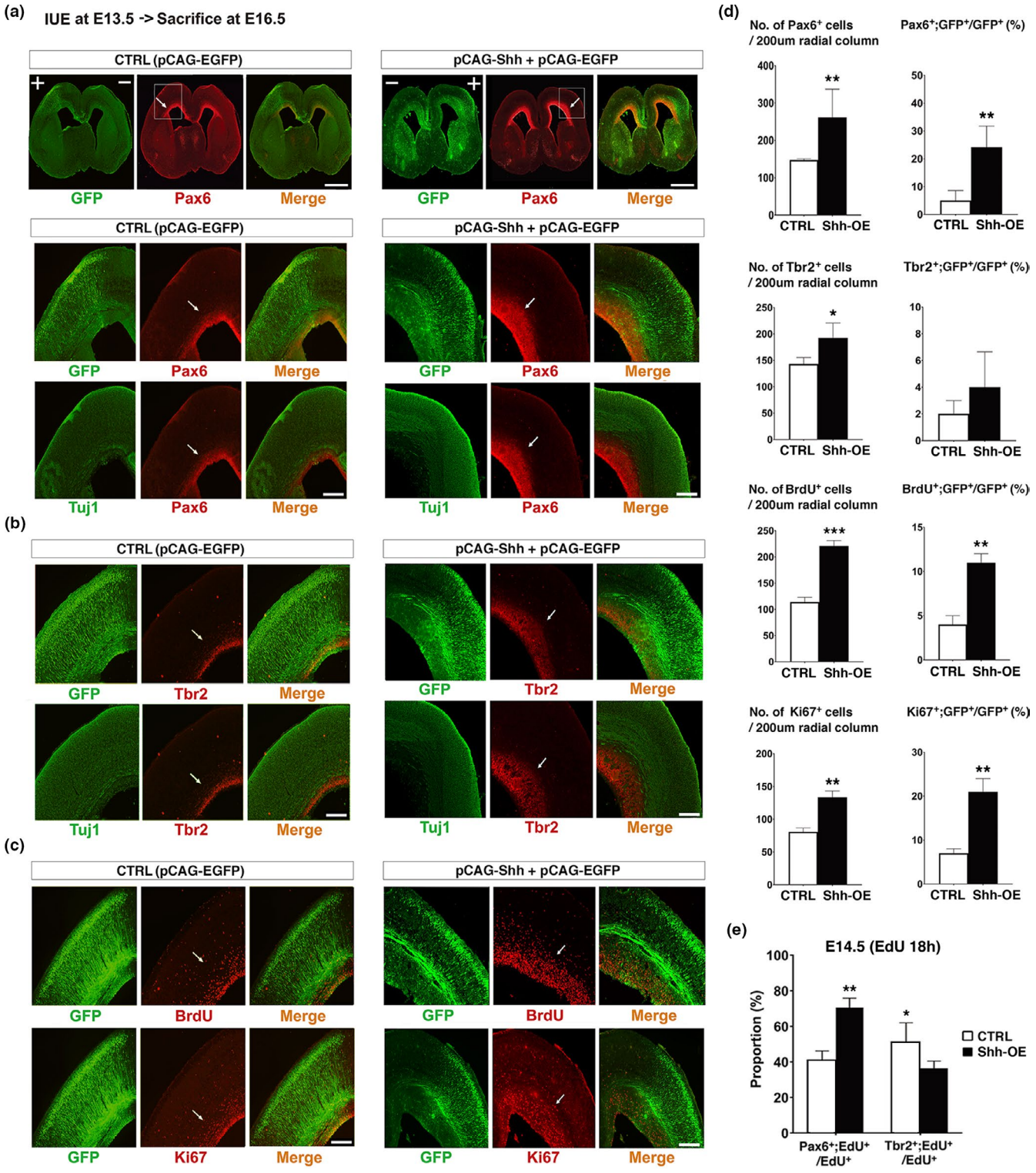

and spinal cord, after the administration of doxycycline (Dox) (Figure 2b,c,e). We obtained several independent Tg lines and performed screening based on Shh/d2EGFP expression levels and patterns. Phenotypes of the Shh-overexpressing Tg mice varied depending on the timing and dosage of Dox administration. In case of Dox administration from earlier stages (from E9.5 or earlier) or with higher concentrations (0.5 mg/ml), Tg embryos frequently showed severe damage in the CNS, including intracranial hemorrhage and neural tube defects such as exencephaly (open brain) and spina bifida (ruptured spinal cord) (Figure S1). With proper timing and dosage of Dox, Tg mice survived and exhibited a bigger brain size compared to that in control (Ctrl) mice at embryonic and postnatal stages (Figure 2b–d and Figure S2a).

To reveal the expression patterns of Shh, we performed double staining using anti-GFP and anti-Shh antibodies and

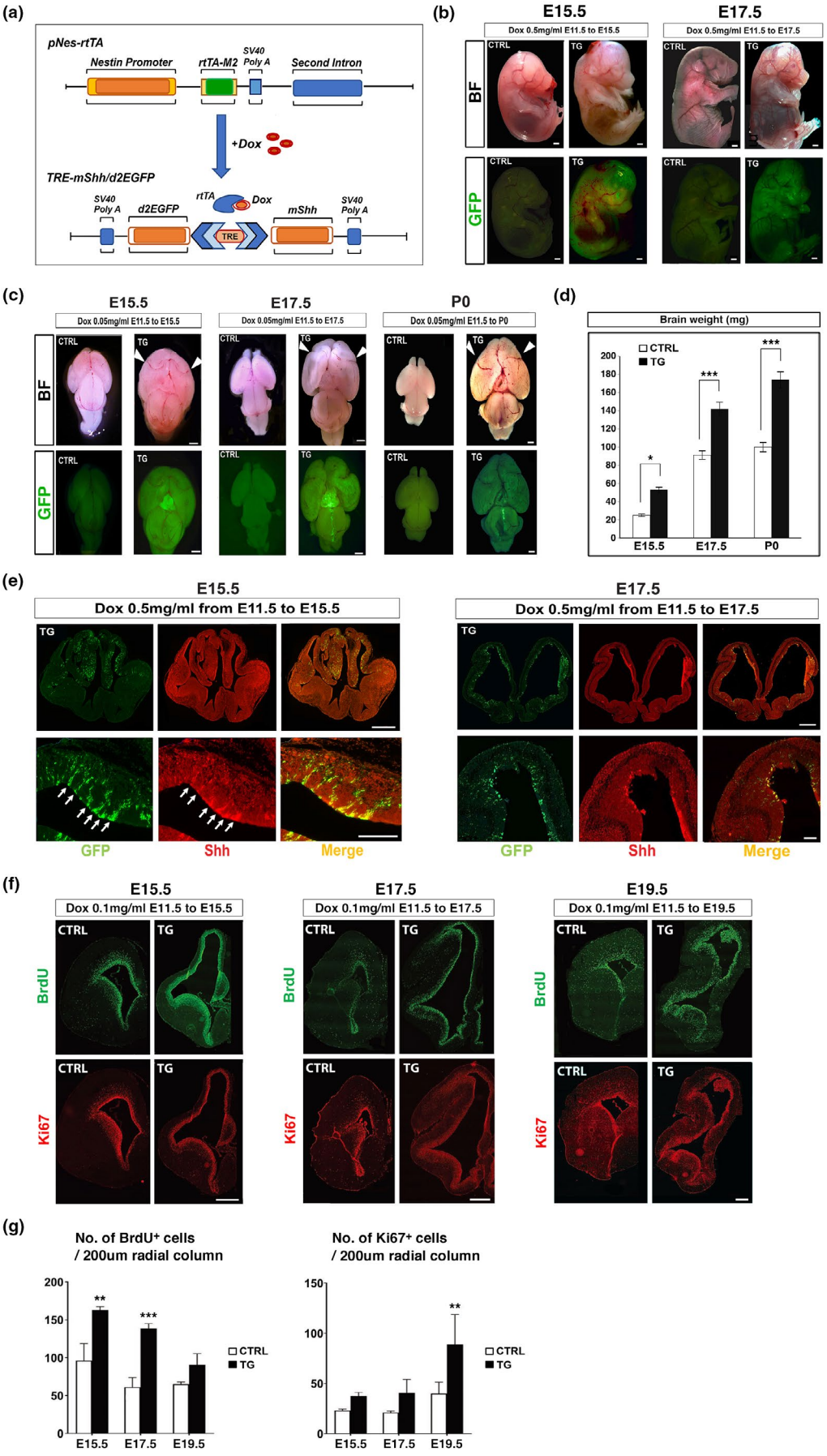
(a)
pNes-rtTA
Nestin Promoter
rtTA-M2
SV40 Poly A
Second Intron
+Dox
TRE-mShh/d2EGFP
SV40 Poly A
d2EGFP
rtTA
Dox
TRE
mShh
SV40 Poly A
(b)
E15.5
Dox 0.5mg/ml E11.5 to E15.5
E17.5
Dox 0.5mg/ml E11.5 to E17.5
BF
GFP
CTRL
TG
(c)
E15.5
Dox 0.05mg/ml E11.5 to E15.5
E17.5
Dox 0.05mg/ml E11.5 to E17.5
P0
Dox 0.05mg/ml E11.5 to P0
BF
GFP
CTRL
TG
(d)
Brain weight (mg)
CTRL
TG
200
180
160
140
120
100
80
60
40
20
0
*
***
***
E15.5
E17.5
P0
(e)
E15.5
Dox 0.5mg/ml from E11.5 to E15.5
E17.5
Dox 0.5mg/ml from E11.5 to E17.5
TG
GFP
Shh
Merge
(f)
E15.5
Dox 0.1mg/ml E11.5 to E15.5
E17.5
Dox 0.1mg/ml E11.5 to E17.5
E19.5
Dox 0.1mg/ml E11.5 to E19.5
BrdU
Ki67
CTRL
TG
(g)
No. of BrdU+ cells
/ 200um radial column
200
150
100
50
0
**
***
CTRL
TG
E15.5
E17.5
E19.5
No. of Ki67+ cells
/ 200um radial column
150
100
50
0
**
CTRL
TG
E15.5
E17.5
E19.5

FIGURE 2 Expansion of neocortical region in Shh-overexpressing Tg mice. (a) Structure of *pNes-rtTA* and *TRE-mShh/d2EGFP* transgenes. Mice generated by crossing both Tg lines bidirectionally expressed mouse Shh (mShh) and the fluorescent reporter d2EGFP in Nestin-expressing cells, including NSCs and neural progenitors, in the presence of doxycycline (Dox). (b) Bright-field (BF) images of whole bodies and GFP expression (green) in Ctrl (CTRL) and Shh-overexpressing Tg (TG) mice at E15.5 and E17.5. Dox was administered from E11.5. (c) Bright-field images of brains and GFP expression (green) in Ctrl and Tg mice at E15.5, E17.5 and postnatal day 0 (P0). Arrowheads indicate bilateral folds on neocortical surface of the Tg brain. (d) A graph showing the brain weights of Ctrl and Tg mice at E15.5, E17.5 and P0. (e) Expression patterns of d2EGFP and Shh. Coronal sections of the telencephalon of E15.5 and E17.5 Tg embryos were double-stained using anti-GFP (green) and anti-Shh (red) antibodies. Arrows indicate double-positive cells in the VZ/SVZ. (f) Analysis of the cell proliferation rate by BrdU incorporation experiments. BrdU was injected intraperitoneally into the pregnant mice 30 min before sacrifice. Coronal sections of the telencephalon of E15.5, E17.5 and E19.5 mice were immunostained using anti-BrdU (green) and anti-Ki67 (red) antibodies. (g) Quantification of the numbers of $BrdU^+$ cells and $Ki67^+$ cells within a radial column of 200 μm width in the neocortical region. Data are mean ± *SEM* ($n = 4$); $^*p < .05$, $^{**}p < .01$, $^{***}p < .001$ (Student's *t* test). Scale bars: 1 mm in b, c, e (upper panels); 500 μm in f; 200 μm in e (lower panels)

found that d2EGFP and Shh were mostly colocalized and that double-positive (GFP^+; Shh^+) cells were sparsely distributed in the VZ and SVZ of the dorsal and ventral telencephalon (Figure 2e). In the Tg brains, the lateral ventricles were dramatically expanded, and the VZ and SVZ of the dorsal telencephalon (neocortical region) were extended tangentially (Figure 2e,f). Accordingly, the morphology of the dorsal telencephalon was severely deformed; further, sometimes many wrinkles or folds were observed on the neocortical surface (Figure 2c,e and Figure S2). Based on the coronal sections of Tg brains, it was revealed that the structure of cortical folding was variable; some mice exhibited a dramatic extension of the germinal layer (VZ) with a tangled cortical wall (Figure S2b), whereas others exhibited the folding of neuronal layers (Figure S2c). These results suggested that Shh secreted from a fraction of VZ/SVZ cells (GFP^+; Shh^+) exerted the non-cell autonomous effect on surrounding cells in broad regions.

We next estimated the cell proliferation rate by performing BrdU incorporation experiments. BrdU was intraperitoneally injected into pregnant mice 30 min before sacrifice at E15.5, E17.5 or E19.5. The numbers of $BrdU^+$ cells in the VZ/SVZ of the neocortical region were significantly higher in the Tg brains than in the Ctrl brains at E15.5 and E17.5 (Figure 2f,g). Immunostaining with antibodies against Ki67 also demonstrated higher numbers of proliferating cells in the neocortical region of Tg mice compared to those in Ctrl mice (Figure 2f,g). These results suggested that secreted Shh influenced NSCs and neural progenitors in broad areas of the neocortical region and promoted cell proliferation, leading to a marked extension of the VZ/SVZ and deformity of the neocortex with wrinkles and folds (Figure 2c,e and Figure S2).

2.3 | NSCs were increased and neuronal differentiation was suppressed in the neocortical region of Shh-overexpressing mice

We next examined the maintenance and differentiation of NSCs and formation of neocortical layers. Immunohistochemical staining using antibodies against Pax6 and Tuj1 demonstrated that the thickness of the $Pax6^+$ cell layer was markedly increased in the neocortical region of Tg brain compared to that in the Ctrl brain (Figure 3a,b). In contrast, the outer cortical layers, including the intermediate zone and cortical plate, were markedly thinner in the Tg brain than in the Ctrl brain. We analyzed the division mode of neural stem/progenitor cells in the neocortical region by the same EdU labeling method as in Figure 1e and observed that many of them continued expansion of the $Pax6^+$ cells in the Tg brain, whereas significantly more cells produced $Tbr2^+$ IPCs in the Ctrl brain (Figure 3c). These results indicated that neuronal differentiation was suppressed in the Tg cortex, and NSCs continued to proliferate via symmetric divisions and tangentially expanded in the neocortical region, leading to extension of the VZ and expansion of lateral ventricles (Figures 2f, 3a).

It has been reported that Shh signaling promotes the proliferation of basal progenitors, including IPCs and basal radial glial cells (bRGCs), in the SVZ of the neocortical region of developing mice (Shimada et al., 2019; Wang et al., 2016), and it is assumed that an increase in these basal progenitors induced the neocortical expansion and folding in gyrencephalic mammals (Borrell & Götz, 2014; Nonaka-Kinoshita et al., 2013). Thus, we performed immunohistochemistry using antibodies against Pax6 and Tbr2. In the neocortical region of Tg brain, $Tbr2^+$ IPCs were sparsely observed and deceased in number, although the number of $Pax6^+$ NSCs was increased compared to that in the Ctrl brain (Figure 3d,e). $Pax6^+$ cells were mostly localized to the VZ, and $Tbr2^+$ cells were distributed more basally in the VZ and SVZ in the Ctrl brain (Figure 3d). In contrast, $Tbr2^+$ cells were encompassed in the expanded $Pax6^+$ cell layer, and thus, many $Pax6^+$ cells were observed at the basal side of the $Tbr2^+$ cell layer in the Tg brain. These results suggested that Shh overexpression led to expansion of $Pax6^+$ NSCs at the expense of $Tbr2^+$ IPCs and impaired the integrity of the VZ/SVZ. bRGCs retain basal processes like apical RGCs (aRGCs) but are detached from the ventricular surface through the loss of apical processes and are located in the SVZ (LaMonica et al., 2012; Wang et al., 2011). They are positive for Pax6 and Sox2 like aRGCs and continue symmetric or asymmetric divisions in the SVZ. To

detect bRGC-like cells, we performed double staining using antibodies against Pax6 and phospho-histone H3 (pH3), a marker of dividing cells. In the Tg brain, we observed many Pax6$^+$ cells dividing at the basal side (Pax6$^+$; pH3$^+$) (Figure 3f,g), but we could not determine the increase in bRGC-like cells located in the SVZ, because the structure of the VZ/SVZ was impaired by Shh overexpression, and the border between the VZ and SVZ became ambiguous (Figure 3a,d).

Shh-overexpressing Tg mice were embryonic lethal when higher concentrations of Dox were administered from

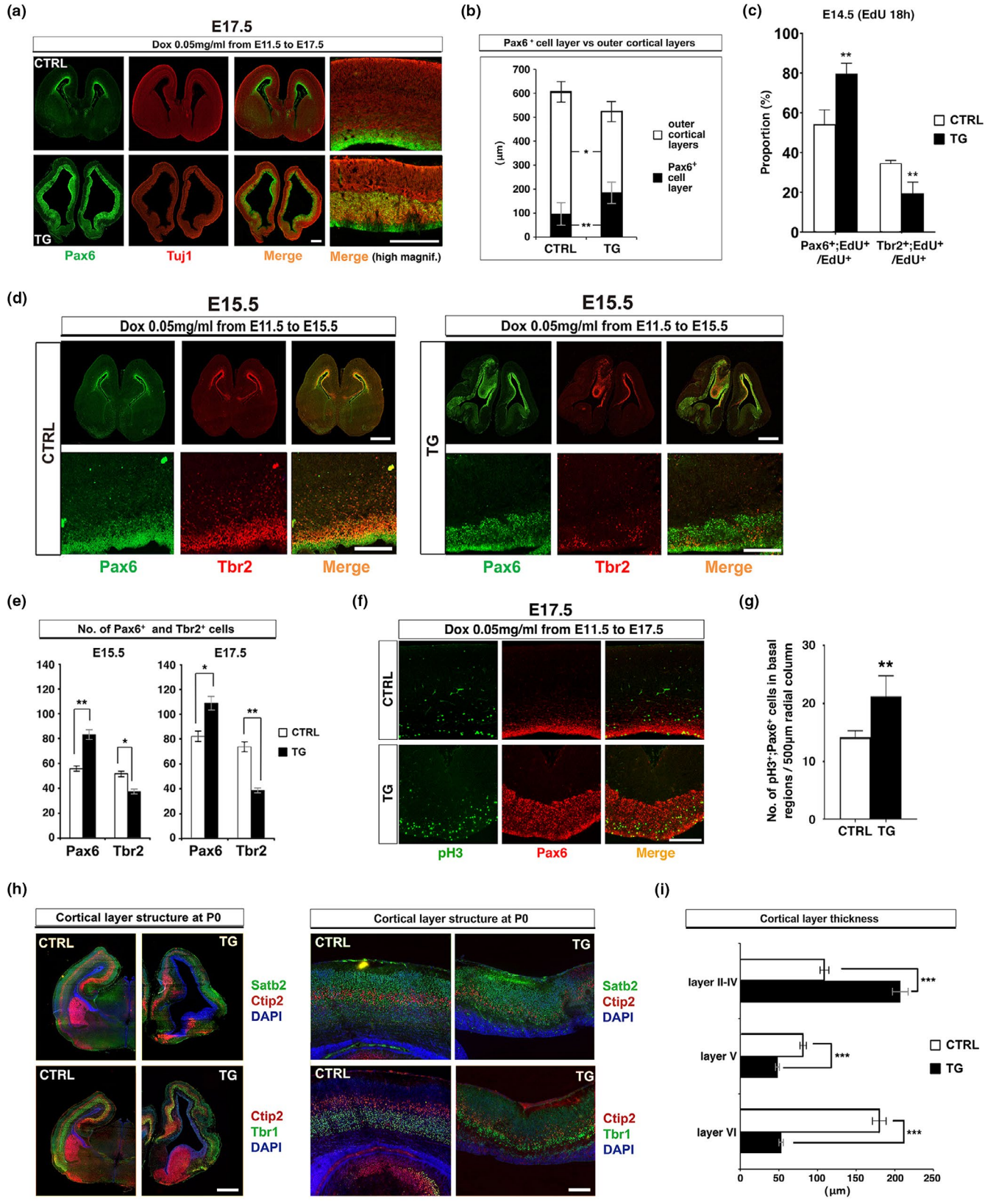

FIGURE 3 Modification in developing germinal layer and postnatal cortical layer structure. (a) Immunostaining with anti-Pax6 (green) and anti-Tuj1 (red) antibodies on coronal sections of the telencephalon of Ctrl and Tg embryos at E17.5. (b) A graph showing the thicknesses of the $Pax6^+$ cell layer and outer cortical layers of the Ctrl and Tg cortices at E17.5. (c) Analysis of the division mode of NSCs. EdU was injected intraperitoneally into pregnant mice, and the proportions of $Pax6^+$; EdU^+/EdU^+ cells and $Tbr2^+$; EdU^+/EdU^+ cells were estimated 18 hr after EdU administration at E14.5. (d) Immunostaining with anti-Pax6 (green) and anti-Tbr2 (red) antibodies on coronal sections of the telencephalon of Ctrl and Tg embryos at E15.5. (e) Quantification of the numbers of $Pax6^+$ and $Tbr2^+$ cells in the VZ/SVZ within a radial column of 200 μm width at E15.5 and E17.5. (f) Double-labeling with anti-pH3 (green) and anti-Pax6 (red) antibodies on coronal sections of the neocortical region at E17.5. (g) Quantification of the numbers of $pH3^+$; $Pax6^+$ cells in basal regions within a radial column of 500 μm width at E17.5. (h) Coronal sections of the Ctrl and Tg brains were immunostained using anti-Satb2 (green), anti-Ctip2 (red) and anti-Tbr1 (green) antibodies at P0. DAPI (blue) represents nuclear staining. Higher magnification views of the cortices are shown in the right panels. (i) Quantification of the thickness of each cortical layer at P0. Data are mean ± *SEM* ($n = 3$); $*p < .05$, $**p < .01$, $***p < .001$ (Student's *t* test). Scale bars: 500 μm in a; 1 mm in d (upper panels), h (left panels); 200 μm in d (lower panels), f, h (right panels)

early embryonic stages. However, when lower concentrations of Dox (<0.05 mg/ml in drinking water) were administered from later embryonic stages, some Tg pups survived until postnatal stages, and mice with milder phenotypes could grow to adulthood. Thus, we next analyzed the neocortical layer formation in postnatal mice using antibodies against Satb2, a marker for layer II-IV neurons, Ctip2, a marker for layer V neurons, and Tbr1, a marker for layer VI neurons. We found that the neocortical layer structure was not severely disturbed, although the deep layers (layers V and VI) were thinner in the Tg neocortex than those in the Ctrl brain, whereas the superficial layers (layer II–IV) were rather thicker than those in the Ctrl neocortex (Figure 3h,i). Shimada et al. reported a similar phenotype in *Gpr161*-mutant mice in which Shh signaling was up-regulated in NSCs of forebrain regions (Shimada et al., 2019).

These results demonstrated that deep layer neurogenesis was more severely affected than superficial layer neurogenesis, but the migration of each layer neurons was not significantly impaired in the Shh-overexpressing Tg neocortex. Most phenotypes of the Shh-overexpressing Tg mice (extension of the ventricular surface, expansion of NSCs, formation of cortical folds, increase in the upper layer and decrease in deep layer neurons) were consistent with those observed in other mutant mice in which Shh signaling was enhanced (Shimada et al., 2019; Wang et al., 2016), but the formation of folding in the neocortical surface was much more prominent in our Tg mice, as shown in Figure 2c and Figure S2.

2.4 | Shh overexpression caused neocortical expansion despite ectopic expression of some ventral marker genes

We observed the marked promotion of NSC proliferation and a dramatic expansion of the VZ/SVZ throughout the neocortical region of Tg brain, although only a subset of cells expressed Shh as shown in Figure 2e. These results suggested that secreted Shh proteins were distributed to surrounding areas through interstitial spaces in the VZ/SVZ or diffused to broader areas via the CSF in lateral ventricles and exerted long-range signaling activity. Thus, we examined how widely Shh signaling was activated by in situ hybridization using RNA probes for Shh signaling components, including *Shh*, *GLI-Kruppel family member GLI1, 2, 3* (*Gli1, 2, 3*), *Patched-1* (*Ptch1*) and *Smoothened* (*Smo*). The expression of *Shh* mRNA was detected in a subset of cells in the VZ/SVZ similar to the expression pattern of Shh proteins shown in Figure 2e (Figure 4a,b and Figure S3a). Quantitative real-time RT-PCR confirmed high levels of *Shh* mRNA expression in the Tg telencephalon at E15.5 and E17.5 after Dox administration starting at E11.5, compared to that in the Ctrl brain (Figure 4c). Notably, we observed higher levels of *Gli1* and *Ptch1* expression in the VZ/SVZ in broad areas of the Tg brain, although the expression levels of *Gli2*, *Gli3* and *Smo* were comparable to those in the Ctrl brain (Figure 4a–c and Figure S3a). These results corroborate the suggestion that Shh proteins produced by a subset of cells were widely distributed and caused the activation of Shh signaling in broad areas, thus expanding NSCs by a non-cell autonomous effect.

It is known that basic helix-loop-helix (bHLH) transcription factors play critical roles in regulating the maintenance and differentiation of NSCs. We previously reported that Hes1 and Hes5, the repressor type of bHLH factors, inhibit neuronal differentiation and maintain the undifferentiated status of NSCs by repressing and counteracting neurogenic bHLH factors, such as Neurog1/2 and Ascl1, in the developing brain (Ohtsuka et al., 1999, 2001). We found that *Hes1* expression was significantly up-regulated in the Shh-overexpressing Tg brain by in situ hybridization and quantitative real-time RT-PCR (Figure 4d–f and Figure S3b). *Neurog2* expression was reduced in the dorsal telencephalon of Tg brains as compared to that in the Ctrl (Figure 4d,e and Figure S3b), although *Neurog2* expression level in the whole telencephalon was slightly increased in the Tg brain (Figure 4g). These results suggested that the up-regulation of *Hes1* led to the inhibition of neuronal differentiation by repressing or counteracting Neurog2 and maintained the proliferation of NSCs in the neocortical

region of Shh-overexpressing mice. It would be of significance to reveal the interactions between Shh signaling and Notch signaling in addition to the previous findings (Kong et al., 2015).

Shh is produced from the floor plate of the neural tube, and Shh signaling is important to promote the ventral fate of the neural tube, including the telencephalon (Kohtz et al., 1998). Moreover, ectopic expression of Shh leads to ventralization in the spinal cord during chicken embryonic development (Echelard et al., 1993; Yang et al., 2019). Thus, we examined whether Shh overexpression exerted a ventralization effect on the developing telencephalon. In the developing brain,

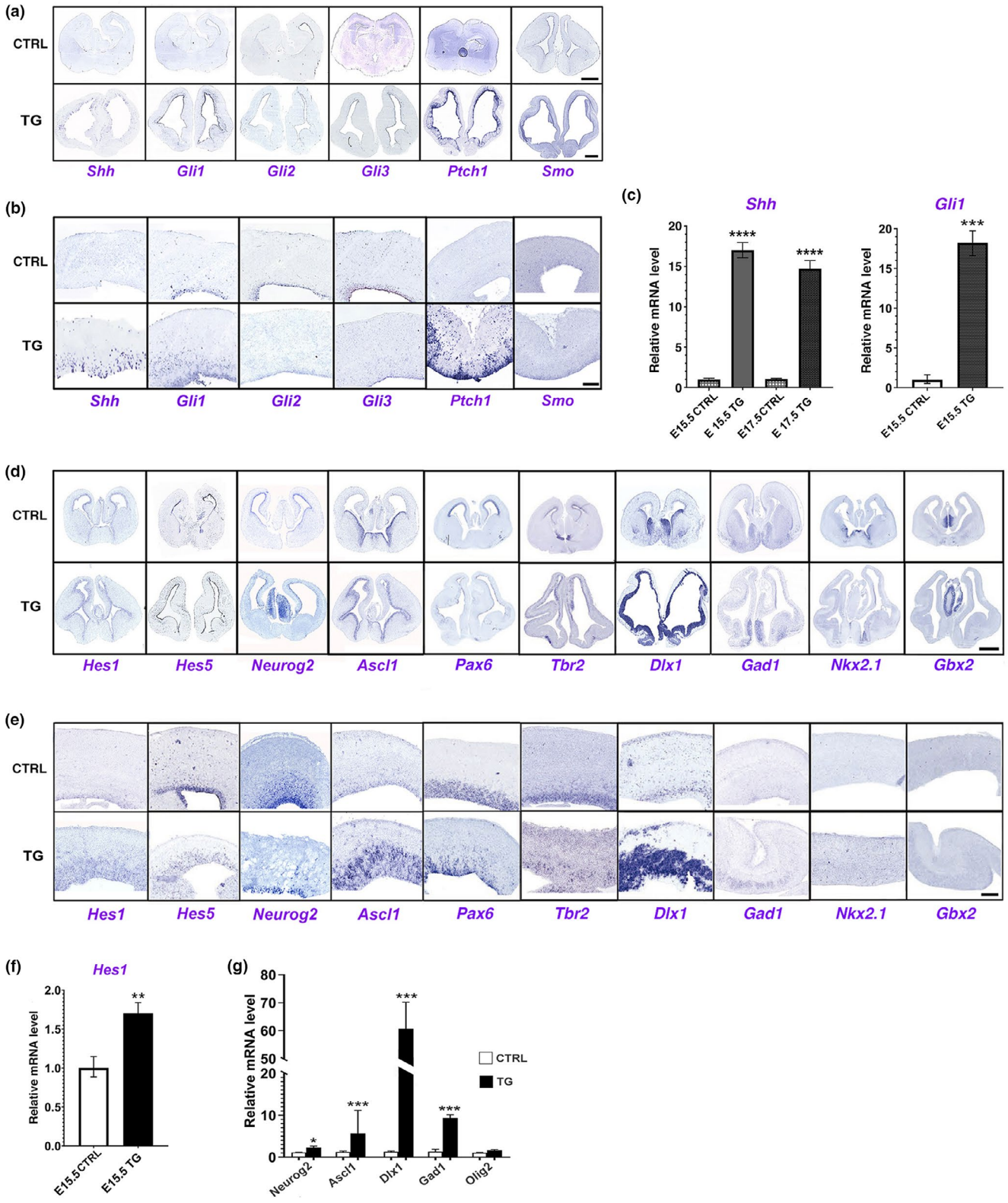

FIGURE 4 Expression patterns of Shh signal components, bHLH genes and D-V markers. (a) Expression patterns of Shh signal components. In situ hybridization for *Shh*, *Gli1*, *Gli2*, *Gli3*, *Ptch1* and *Smo* was performed on coronal sections of the Ctrl and Tg brains at E17.5. (b) Higher magnification views of neocortical areas showing mRNA expression of Shh signal components. (c) Quantitative real-time RT-PCR using total RNAs prepared from the whole telencephalon of Ctrl and Tg embryos. Dox was administered from E11.5 onward. Expression levels of *Shh* were compared between the Ctrl and Tg brains at E15.5 and E17.5. *Gli1* expression was examined at E15.5. *Gapdh* was used as an internal control, and the values were normalized to those of the Ctrl sample. (d) Expression patterns of various bHLH genes and ventral marker genes. In situ hybridization for *Hes1*, *Hes5*, *Neurog2*, *Ascl1*, *Pax6*, *Tbr2*, *Dlx1*, *Gad1*, *Nkx2.1 and Gbx2* was performed on coronal sections of the Ctrl and Tg brains at E17.5. (e) Higher magnification views of neocortical areas showing mRNA expression of bHLH genes and ventral marker genes. (f) Quantitative real-time RT-PCR using total RNAs prepared from the whole telencephalon of Ctrl and Tg embryos. Dox was administered from E11.5 onward. Expression levels of *Hes1* were compared between the Ctrl and Tg brains at E15.5. (g) Quantitative real-time RT-PCR using total RNAs prepared from the whole telencephalon of Ctrl and Tg embryos. Dox was administered from E11.5 onward. Expression levels of *Neurog2*, *Ascl1*, *Dlx1*, *Gad1* and *Olig2* were examined at E15.5. *Gapdh* was used as an internal control, and the values were normalized to those of the Ctrl sample. Data are mean ± *SEM* ($n = 8$ for *Gli1* and *Hes1*; $n = 4$ for other genes); $*p < .05$, $**p < .01$, $***p < .001$, $****p < .0001$ (Student's *t* test). Scale bars: 1 mm in a, d; 200 μm in b, e

Neurog1/2 is expressed in the dorsal telencephalon and induces excitatory glutamatergic neurons. In contrast, *Ascl1* is predominantly expressed in the ventral telencephalon and induces GABAergic inhibitory interneurons (Guillemot & Joyner, 1993; Porteus et al., 1994; Sommer et al., 1996; Toresson et al., 2000). Therefore, we analyzed the expression patterns and levels of several D-V marker genes, such as *Neurog2*, *Ascl1*, *Pax6*, *Tbr2, Dlx1*, *Gad1*, *Nkx2.1*, *Gbx2* and *Olig2*. In contrast to that of *Neurog2*, the expression of *Ascl1* was significantly up-regulated in the dorsal telencephalon of Tg brains compared to that in the Ctrl (Figure 4d,e,g and Figure S3b). Furthermore, we found markedly higher expression levels of *Dlx1* and significantly higher levels of *Gad1*, both of which are expressed in the ventral telencephalon of Ctrl mice, ectopically in the dorsal telencephalon of the Shh-overexpressing Tg mice, although the ectopic expression of other ventral marker genes such as *Nkx2.1* and *Gbx2* was not observed in the dorsal telencephalon (Figure 4d,e and Figure S3b). It was reported that *Dlx1* expression is up-regulated in accordance with the up-regulation of *Ascl1* in the dorsal telencephalon of *Neurog1*; *Neurog2* double mutant mice (Fode et al., 2000). These results suggested that Shh overexpression enhanced the expression of *Ascl1* and ventral marker genes instead of *Neurog2* expression in the dorsal telencephalon. However, dorsal marker genes such as *Pax6* and *Tbr2* were substantially expressed in the dorsal telencephalon, although their expression levels were reduced compared to those in the Ctrl brain.

Our results together indicated that Shh overexpression after around E11.5 could lead to neocortical expansion with an increase in cells positive for Pax6, a marker of NSCs of the neocortical region. Those NSCs were capable of producing cortical layer neurons and formed orderly cortical layers (Figure 3h), without inducing a drastic disturbance in D-V patterning, as shown by the expression of Pax6, Tbr1 and Tbr2 in the dorsal telencephalon (Figures 3d,h and 4d,e and Figure S2b,c), even though some ventral marker genes were ectopically expressed in the dorsal telencephalon.

Increasing evidence has revealed that Shh promotes cell proliferation of various types of neural cells, such as granule neuron precursors in the cerebellum (Wallace, 1999), NSCs in the developing dorsal midbrain (Martínez et al., 2013) and NSCs in the postnatal and adult forebrain SVZ (Palma et al., 2005). However, there have been few studies that demonstrated the impact of Shh on neocortical NSCs and progenitors in the developing brain. Most of the previous studies reported the effect of Shh on promoting the proliferation of neocortical progenitors through in vitro experiments (Komada et al., 2008), in utero electroporation (Shikata et al., 2011) or analyses of deletion mutants of Shh signaling components (Dave et al., 2011; Komada et al., 2008; Machold et al., 2003; Palma & Ruiz i Altaba, 2004; Shikata et al., 2011; Xu et al., 2005). Dave et al. reported that the activation of Shh signaling at early stages of neocortical development resulted in an increase in symmetric proliferative divisions of NSCs in *Ptch1*-mutant mice (Dave et al., 2011). In addition, it was reported that the overexpression of a constitutively active form of Smoothened (SmoM2), an effector of Shh signaling, in the mutant mice (*GFAP::Cre; SmoM2*$^{fl/+}$) caused enlargement of the neocortical surface (Wang et al., 2016). However, in either case, the neocortical expansion and folding were not prominent due to the difficulty in controlling the levels of Shh signaling. In contrast, our system enabled control of the timing and levels of Shh expression, which are critical for brain morphology and embryonic lethality, by modulating the Dox dosage in drinking water, and thus succeeded in the acquisition of a prominently enlarged neocortical surface with complicated wrinkles and folds. These results suggested that enhanced activation of Shh signaling during neocortical development might have contributed to mammalian brain evolution.

3 | EXPERIMENTAL PROCEDURES

3.1 | Plasmid construction and in utero electroporation

Polymerase chain reaction (PCR) fragments of mouse *Shh* coding sequence from cDNA Library with or without

hemagglutinin (HA)-tag sequences were cloned into the *pCAG* expression vector driven by the *CAG* promoter (*pCAG-Shh*). *Enhanced green fluorescent protein (EGFP)* linked to the *CAG* promoter (*pCAG-EGFP*) was used as a control vector and as a reporter when co-transfected with *pCAG-Shh* plasmid vector. In utero electroporation was performed at E13.5 using methods described previously (Ohtsuka et al., 2011). Embryos were harvested 3 days after electroporation at E16.5. Brains were excised, fixed in 4% paraformaldehyde, cryoprotected, embedded in OCT and cryosectioned at 16 μm.

3.2 | Immunohistochemistry

Immunohistochemistry was performed as described previously (Ohtsuka et al., 2011). Brains were fixed in 4% paraformaldehyde, incubated overnight with 20%–25% (w/v) sucrose in PBS at 4°C, embedded in OCT compound and cryosectioned coronally at 16 μm thickness. Sections were blocked with 5% normal goat or donkey serum/0.1% Triton X-100 in PBS for 1 hr at room temperature. Primary antibodies diluted in 1% normal goat or donkey serum/0.1% Triton X-100 in PBS were applied overnight at 4°C. Primary antibodies used in this study are listed in Table S1. Alexa Fluor-conjugated secondary antibodies (Molecular Probes; 1:200) were applied for 2 hr at room temperature to detect primary antibodies. DAPI (4′,6-diamidino-2-phenylindole; Sigma-Aldrich) was used for nuclear staining. Images were analyzed using all-in-one fluorescence microscope BZ-X800 (Keyence).

3.3 | BrdU incorporation assay

5-Bromo-2′-deoxyuridine (BrdU; Sigma-Aldrich; 50 μg BrdU/g of body weight) was injected intraperitoneally to pregnant mice 30 min before sacrifice. The $BrdU^+$ cells were detected by immunohistochemistry as described previously (Tan et al., 2012).

3.4 | Generation of Shh-overexpressing mice

For the *pNes-rtTA* transgene, a *rtTA-Advanced* fragment excised from *pTet-On Advanced* vector (Clontech) was subcloned between the *Nes* promoter (5.8 kb) and polyadenylation sequence of *SV40* with the second intron (1.7 kb) of *Nes* gene (Bansod et al., 2017). For the *TRE-mShh/d2EGFP* transgene, mouse *Shh* and *d2EGFP* (Clontech) cDNAs were inserted into the *pTRE-Tight-BI* vector (Clontech). Three Tg mouse lines were generated using each transgene and maintained on the ICR background. Both lines were crossed and doxycycline hyclate (Sigma-Aldrich; Doxycycline concentration varied from 0.025 to 0.5 mg/ml) in drinking water with 5% sucrose was continuously administered to pregnant mice from E11.5 or E12.5 until sacrifice. Images of whole bodies and brains with GFP fluorescence were obtained with a MZ16FA fluorescence stereo microscope equipped with a DFC300 FX digital camera (Leica). Animal experiments were carried out according to the guidelines for animal experiments at Kyoto University.

3.5 | Estimation of symmetric versus asymmetric division mode

To estimate the division mode (symmetric versus asymmetric division) of transfected cells, in utero electroporation was performed at E13.5. 5-Ethynyl-2′-deoxyuridine (EdU; Thermo Fisher Scientific; 12.5 μg EdU/g of body weight) was injected intraperitoneally into pregnant mice 12 hr after in utero electroporation, and mice were sacrificed 18 hr after EdU injection at E14.5. To estimate the division mode of NSCs in the Shh-overexpressing Tg versus control mice, EdU (12.5 μg EdU/g of body weight) was injected intraperitoneally into pregnant mice, and mice were sacrificed 18 hr after EdU injection at E14.5. The numbers of $Pax6^+$; EdU^+/EdU^+ cells and $Tbr2^+$; EdU^+/EdU^+ cells were counted within a radial column of 200 μm width on the coronal sections of the neocortical region.

3.6 | In situ hybridization

Preparation of digoxigenin-labeled RNA probes and in situ hybridization were performed as described previously (Ohtsuka et al., 2011). The coding sequences of *Shh* (NM_009170.3), *Gli1* (NM_010296.2), *Gli2* (NM_001081125.1), *Gli3* (NM_008130.3),*Ptch1*(NM_008957.3),*Smo*(NM_176996.4), *Hes1* (NM_008235.2), *Hes5* (NM_010419.4), *Neurog2* (NM_009718.3), *Ascl1* (NM_008553.4), *Pax6* (NM_001244198.2), *Tbr2* (NM_010136.3), *Dlx1* (NM_010053.2), *Gad1* (NM_001312900.1), *Nkx2.1* (NM_009385.3) and *Gbx2* (NM_010262.3) were used as templates for the RNA probes. RNA probes were synthesized in vitro using the full- or partial-length cDNAs cloned into the *pTA2/pBS/pGEM/pCR* vectors.

3.7 | Quantitative real-time RT-PCR

Total RNA was prepared from the whole telencephalon of mouse embryos with QIAGEN RNeasy kit. Reverse transcription was performed using total RNA as described previously (Tan et al., 2012). KOD SYBR qPCR Mix (TOYOBO)

and 10 μM primers were used in each reaction. PCR was performed with Step-One machine (ABI). *Gapdh* was used as an internal control. PCR primers are listed in Table S2.

3.8 | Cell count

Cell numbers within a radial column of 200 μm (Figures 1d, 2g, 3e) or 500 μm (Figure 3g) width in the neocortical region were counted on the coronal sections.

3.9 | Statistical analysis

Each value was obtained from at least three independent samples. Statistical significance was evaluated by Student's *t* test. Data are presented as mean ± *SEM*.

ACKNOWLEDGEMENTS

We thank Hitoshi Miyachi and Satsuki Kitano for their help in the generation of *TRE-mShh/d2EGFP* transgenic mice. This work was supported by Core Research for Evolutional Science and Technology [JPMJCR12W2 to R.K.], Grant-in-Aid for Scientific Research on Innovative Areas from the Ministry of Education, Culture, Sports, Science and Technology (MEXT) [16H06480 to R.K.], and Grant-in-Aid for Scientific Research from the Japan Society for the Promotion of Science (JSPS) [15K06773 and 18K06253 to T.O.].

ORCID

Toshiyuki Ohtsuka https://orcid.org/0000-0001-6045-1012

REFERENCES

Bansod, S., Kageyama, R., & Ohtsuka, T. (2017). Hes5 regulates the transition timing of neurogenesis and gliogenesis in mammalian neocortical development. *Development*, *144*(17), 3156–3167. https://doi.org/10.1242/dev.147256

Borrell, V., & Götz, M. (2014). Role of radial glial cells in cerebral cortex folding. *Current Opinion in Neurobiology*, *27*, 39–46. https://doi.org/10.1016/j.conb.2014.02.007. Epub 2014 Mar 12.

Chiang, C., Litingtung, Y., Lee, E., Young, K. E., Corden, J. L., Westphal, H., & Beachy, P. A. (1996). Cyclopia and defective axial patterning in mice lacking Sonic hedgehog gene function. *Nature*, *383*(6599), 407–413. https://doi.org/10.1038/383407a0

Dale, J. K., Vesque, C., Lints, T. J., Sampath, T. K., Furley, A., Dodd, J., & Placzek, M. (1997). Cooperation of BMP7 and SHH in the induction of forebrain ventral midline cells by prechordal mesoderm. *Cell*, *90*(2), 257–269. https://doi.org/10.1016/S0092-8674(00)80334-7

Dave, R. K., Ellis, T., Toumpas, M. C., Robson, J. P., Julian, E., Adolphe, C., Bartlett, P. F., Cooper, H. M., Reynolds, B. A., & Wainwright, B. J. (2011). Sonic hedgehog and notch signaling can cooperate to regulate neurogenic divisions of neocortical progenitors. *PLoS One*, *6*(2), e14680. https://doi.org/10.1371/journal.pone.0014680

Echelard, Y., Epstein, D. J., St-Jacques, B., Shen, L., Mohler, J., McMahon, J. A., & McMahon, A. P. (1993). Sonic hedgehog, a member of a family of putative signaling molecules, is implicated in the regulation of CNS polarity. *Cell*, *75*(7), 1417–1430. https://doi.org/10.1016/0092-8674(93)90627-3

Ericson, J., Muhr, J., Placzek, M., Lints, T., Jessell, T. M., & Edlund, T. (1995). Sonic hedgehog induces the differentiation of ventral forebrain neurons: A common signal for ventral patterning within the neural tube. *Cell*, *81*(5), 747–756. https://doi.org/10.1016/0092-8674(95)90536-7

Fode, C., Ma, Q., Casarosa, S., Ang, S. L., Anderson, D. J., & Guillemot, F. (2000). A role for neural determination genes in specifying the dorsoventral identity of telencephalic neurons. *Genes & Development*, *14*(1), 67–80.

Fuccillo, M., Joyner, A. L., & Fishell, G. (2006). Morphogen to mitogen: The multiple roles of hedgehog signalling in vertebrate neural development. *Nature Reviews Neuroscience*, *7*(10), 772–783. https://doi.org/10.1038/nrn1990

Guillemot, F., & Joyner, A. L. (1993). Dynamic expression of the murine Achaete-Scute homologue Mash-1 in the developing nervous system. *Mechanisms of Development*, *42*(3), 171–185. https://doi.org/10.1016/0925-4773(93)90006-J

Kohtz, J. D., Baker, D. P., Corte, G., & Fishell, G. (1998). Regionalization within the mammalian telencephalon is mediated by changes in responsiveness to Sonic Hedgehog. *Development*, *125*(24), 5079–5089.

Komada, M., Iguchi, T., Takeda, T., Ishibashi, M., & Sato, M. (2013). Smoothened controls cyclin D2 expression and regulates the generation of intermediate progenitors in the developing cortex. *Neuroscience Letters*, *547*, 87–91. https://doi.org/10.1016/j.neulet.2013.05.006

Komada, M., Saitsu, H., Kinboshi, M., Miura, T., Shiota, K., & Ishibashi, M. (2008). Hedgehog signaling is involved in development of the neocortex. *Development*, *135*(16), 2717–2727. https://doi.org/10.1242/dev.015891

Kong, J. H., Yang, L., Dessaud, E., Chuang, K., Moore, D. M., Rohatgi, R., Briscoe, J., & Novitch, B. G. (2015). Notch activity modulates the responsiveness of neural progenitors to Sonic hedgehog signaling. *Developmental Cell*, *33*(4), 373–387. https://doi.org/10.1016/j.devcel.2015.03.005

LaMonica, B. E., Lui, J. H., Wang, X., & Kriegstein, A. R. (2012). OSVZ progenitors in the human cortex: An updated perspective on neurodevelopmental disease. *Current Opinion in Neurobiology*, *22*(5), 747–753. https://doi.org/10.1016/j.conb.2012.03.006. Epub 2012 Apr 7.

Machold, R., Hayashi, S., Rutlin, M., Muzumdar, M. D., Nery, S., Corbin, J. G., Gritli-Linde, A., Dellovade, T., Porter, J. A., Rubin, L. L., Dudek, H., McMahon, A. P., & Fishell, G. (2003). Sonic hedgehog is required for progenitor cell maintenance in telencephalic stem cell niches. *Neuron*, *39*(6), 937–950. https://doi.org/10.1016/s0896-6273(03)00561-0

Martínez, C., Cornejo, V. H., Lois, P., Ellis, T., Solis, N. P., Wainwright, B. J., & Palma, V. (2013). Proliferation of murine midbrain neural stem cells depends upon an endogenous Sonic hedgehog (Shh) source. *PLoS One*, *8*(6), e65818. https://doi.org/10.1371/journal.pone.0065818. Print 2013.

Nonaka-Kinoshita, M., Reillo, I., Artegiani, B., Martínez-Martínez, M. Á., Nelson, M., Borrell, V., & Calegari, F. (2013). Regulation of cerebral cortex size and folding by expansion of basal

progenitors. *EMBO Journal*, *32*(13), 1817–1828. https://doi.org/10.1038/emboj.2013.96. Epub 2013 Apr 26.

Ohtsuka, T., Ishibashi, M., Gradwohl, G., Nakanishi, S., Guillemot, F., & Kageyama, R. (1999). Hes1 and Hes5 as notch effectors in mammalian neuronal differentiation. *EMBO Journal*, *18*, 2196–2207. https://doi.org/10.1093/emboj/18.8.2196

Ohtsuka, T., Sakamoto, M., Guillemot, F., & Kageyama, R. (2001). Roles of the basic helix-loop-helix genes Hes1 and Hes5 in expansion of neural stem cells of the developing brain. *Journal of Biological Chemistry*, *276*, 30467–30474. https://doi.org/10.1074/jbc.M102420200

Ohtsuka, T., Shimojo, H., Matsunaga, M., Watanabe, N., Kometani, K., Minato, N., & Kageyama, R. (2011). Gene expression profiling of neural stem cells and identification of regulators of neural differentiation during cortical development. *Stem Cells*, *29*, 1817–1828. https://doi.org/10.1002/stem.731

Palma, V., Lim, D. A., Dahmane, N., Sánchez, P., Brionne, T. C., Herzberg, C. D., Gitton, Y., Carleton, A., Alvarez-Buylla, A., & Ruiz i Altaba, A. (2005). Sonic hedgehog controls stem cell behavior in the postnatal and adult brain. *Development*, *132*(2), 335–344. https://doi.org/10.1242/dev.01567. Epub 2004 Dec 16.

Palma, V., & Ruiz i Altaba, A. (2004). Hedgehog-GLI signaling regulates the behavior of cells with stem cell properties in the developing neocortex. *Development*, *131*(2), 337–345. https://doi.org/10.1242/dev.00930. Epub 2003 Dec 17.

Patten, I., & Placzek, M. (2000). The role of Sonic hedgehog in neural tube patterning. *Cellular and Molecular Life Sciences*, *57*(12), 1695–1708. https://doi.org/10.1007/PL00000652

Porteus, M. H., Bulfone, A., Liu, J. K., Puelles, L., Lo, L. C., & Rubenstein, J. L. (1994). DLX-2, MASH-1, and MAP-2 expression and bromodeoxyuridine incorporation define molecularly distinct cell populations in the embryonic mouse forebrain. *Journal of Neuroscience*, *14*(11 Pt 1), 6370–6383. https://doi.org/10.1523/JNEUROSCI.14-11-06370.1994

Shikata, Y., Okada, T., Hashimoto, M., Ellis, T., Matsumaru, D., Shiroishi, T., Ogawa, M., Wainwright, B., & Motoyama, J. (2011). Ptch1-mediated dosage-dependent action of Shh signaling regulates neural progenitor development at late gestational stages. *Developmental Biology*, *349*(2), 147–159. https://doi.org/10.1016/j.ydbio.2010.10.014

Shimada, I. S., Somatilaka, B. N., Hwang, S. H., Anderson, A. G., Shelton, J. M., Rajaram, V., Konopka, G., & Mukhopadhyay, S. (2019). Derepression of Sonic hedgehog signaling upon Gpr161 deletion unravels forebrain and ventricular abnormalities. *Developmental Biology*, *450*(1), 47–62. https://doi.org/10.1016/j.ydbio.2019.03.011. Epub 2019 Mar 23.

Sommer, L., Ma, Q., & Anderson, D. J. (1996). Neurogenins, a novel family of atonal-related bHLH transcription factors, are putative mammalian neuronal determination genes that reveal progenitor cell heterogeneity in the developing CNS and PNS. *Molecular and Cellular Neurosciences*, *8*(4), 221–241. https://doi.org/10.1006/mcne.1996.0060

Sun, T., & Hevner, R. F. (2014). Growth and folding of the mammalian cerebral cortex: From molecules to malformations. *Nature Reviews Neuroscience*, *15*(4), 217–232. https://doi.org/10.1038/nrn3707

Tan, S. L., Nishi, M., Ohtsuka, T., Matsui, T., Takemoto, K., Kamio-Miura, A., Aburatani, H., Shinkai, Y., & Kageyama, R. (2012). Essential roles of the histone methyltransferase ESET in the epigenetic control of neural progenitor cells during development. *Development*, *139*, 3806–3816. https://doi.org/10.1242/dev.082198

Toresson, H., Potter, S. S., & Campbell, K. (2000). Genetic control of dorsal-ventral identity in the telencephalon: Opposing roles for Pax6 and Gsh2. *Development*, *127*(20), 4361–4371.

Wallace, V. A. (1999). Purkinje-cell-derived Sonic hedgehog regulates granule neuron precursor cell proliferation in the developing mouse cerebellum. *Current Biology*, *9*(8), 445–448. https://doi.org/10.1016/S0960-9822(99)80195-X

Wang, L., Hou, S., & Han, Y. G. (2016). Hedgehog signaling promotes basal progenitor expansion and the growth and folding of the neocortex. *Nature Neuroscience*, *19*(7), 888–896. https://doi.org/10.1038/nn.4307

Wang, X., Tsai, J. W., LaMonica, B., & Kriegstein, A. R. (2011). A new subtype of progenitor cell in the mouse embryonic neocortex. *Nature Neuroscience*, *14*, 555–561. https://doi.org/10.1038/nn.2807

Watanabe, N., Kageyama, R., & Ohtsuka, T. (2015). Hbp1 regulates the timing of neuronal differentiation during cortical development by controlling cell cycle progression. *Development*, *142*(13), 2278–2290. https://doi.org/10.1242/dev.120477

Xu, Q., Wonders, C. P., & Anderson, S. A. (2005). Sonic hedgehog maintains the identity of cortical interneuron progenitors in the ventral telencephalon. *Development*, *132*(22), 4987–4998. https://doi.org/10.1242/dev.02090

Yabut, O. R., & Pleasure, S. J. (2018). Sonic hedgehog signaling rises to the surface: Emerging roles in neocortical development. *Brain Plasticity*, *3*(2), 119–128. https://doi.org/10.3233/BPL-180064

Yang, C., Li, S., Li, X., Li, H., Li, Y., Zhang, C., & Lin, J. (2019). Effect of sonic hedgehog on motor neuron positioning in the spinal cord during chicken embryonic development. *Journal of Cellular and Molecular Medicine*, *23*(5), 3549–3562. https://doi.org/10.1111/jcmm.14254

SUPPORTING INFORMATION

Additional supporting information may be found online in the Supporting Information section.

How to cite this article: Shqirat M, Kinoshita A, Kageyama R, Ohtsuka T. Sonic hedgehog expands neural stem cells in the neocortical region leading to an expanded and wrinkled neocortical surface. *Genes Cells*. 2021;00:1–12. https://doi.org/10.1111/gtc.12847